Performance Studies of Various Cracking Catalysts in the Conversion of Canola Oil to Fuels and Chemicals in a Fluidized-Bed Reactor

Sai P.R. Katikaneni, John D. Adjaye, Raphael O. Idem, and Narendra N. Bakhshi*

Catalysis and Chemical Reaction Engineering Laboratory, Department of Chemical Engineering,
University of Saskatchewan, Saskatoon, Saskatchewan, S7N 5C9 Canada

ABSTRACT: Studies were conducted at atmospheric pressure at temperatures in the range of 400–500°C and fluidizing gas velocities in the range of 0.37–0.58 m/min (at standard temperature and pressure) to evaluate the performance of various cracking catalysts for canola oil conversion in a fluidized-bed reactor. Results show that canola oil conversions were high (in the range of 78–98 wt%) and increased with an increase in both temperature and catalyst acid site density and with a decrease in fluidizing gas velocity. The product distribution mostly consisted of hydrocarbon gases in the C_1–C_5 range, a mixture of aromatic and aliphatic hydrocarbons in the organic liquid product (OLP) and coke. The yields of C_4 hydrocarbons, aromatic hydrocarbons and C_2–C_4 olefins increased with both temperature and catalyst acid site density but decreased with an increase in fluidizing gas velocity. In contrast, the yields of aliphatic and C_5 hydrocarbons followed trends completely opposite to those of C_2–C_4 olefins and aromatic hydrocarbons. A comparison of performance of the catalysts in a fluidized-bed reactor with earlier work in a fixed-bed reactor showed that selectivities for formation of both C_5 and *iso*-C_4 hydrocarbons in a fluidized-bed reactor were extremely high (maximum of 68.7 and 18 wt% of the gas product) as compared to maximum selectivities of 18 and 16 wt% of the gas product, respectively, in the fixed-bed reactor. Also, selectivity for formation of gas products was higher for runs with the fluidized-bed reactor than for those with the fixed-bed reactor, whereas the selectivity for OLP was higher with the fixed-bed reactor. Furthermore, both temperature and catalyst determined whether the fractions of aromatic hydrocarbons in the OLP were higher in the fluidized-bed or fixed-bed reactor.

JAOCS 75, 381–391 (1998).

KEY WORDS: Canola oil conversion, fluidized-bed, HZSM-5, product distribution, silica-alumina.

Biomass is attracting increasing interest as a renewable source for the production of various fuels and chemicals (1–14). It is well known that, unlike petroleum oils, biomass-derived oils, such as bio-crude obtained from wood, vegetable oils and animal fats, do not contain either metals (such as nickel or vanadium) or hetero-atoms (such as nitrogen and sulfur). As such, the upgrading of bio-oils to useful products does not involve the release of pollutants, such as NO_X, SO_X and metal particles, into the atmosphere. Also, the production and upgrading of bio-oils is CO_2 neutral (1). Furthermore, bio-crude upgrading presents a strong potential for the production of fuels and chemicals from waste materials, such as sewage sludge (4), waste vegetable oils from fast-food restaurants and rendering plants (13,14), and tall oil from Kraft and pulping operations (5,9). Thus, all these studies show that bio-crudes are not just a renewable resource but also that their upgrading to fuels and chemicals is environmentally benign.

In earlier studies (12–20), the catalytic upgrading of canola oil (used as a model compound to represent waste vegetable oils from fast-food restaurants and rendering plants) was studied in a fixed-bed reactor over various cracking catalysts, namely HZSM-5, silicalite, HY, H-mordenite, aluminum-pillared clays, silica-alumina, γ-alumina and silica-alumino phosphates, to determine the effects of catalyst characteristics (such as acidity and acid site distribution, basicity, shape selectivity, crystallinity, pore size, and pore size distribution) on oil conversion and product distribution as well as to study thermal stability of the catalysts under various operating environments. These studies showed that overall oil conversion and yields of individual products were unique for each type of catalyst. For example, under the operating conditions used, high yields of aromatic hydrocarbons were obtained with shape-selective catalysts, such as HZSM-5 and silicalite, whereas high yields of aliphatic hydrocarbons were obtained for nonshape-selective catalysts, such as silica-alumina and γ-alumina.

Also, in a recent study (16), the use of HS-Mix (a catalyst consisting of a physical mixture of HZSM-5 and silica-alumina) for the upgrading of a wood-derived bio-crude resulted in high selectivity for isooctane. In contrast, the use of HS-Mix catalyst for canola oil conversion resulted only in high selectivity for C_2–C_4 olefins (14). On the other hand, conversion of canola oil over a different type of modified HZSM-5 catalyst (i.e., by impregnation with potassium) resulted in an increase in the yield of C_2–C_4 olefins and a corresponding decrease in the yield of aromatic hydrocarbons (17). In contrast, the use of platinum-impregnated HZSM-5 catalysts for canola oil conversion did not result in any changes in yield of aro-

---

*To whom correspondence should be addressed.
E-mail: burlock@engr.usask.ca.

matic hydrocarbons or composition of the organic liquid product (OLP) from those obtained with nonimpregnated HZSM-5. However, there was a tremendous improvement in selectivity for iso-hydrocarbons, such as isobutane and isobutylene, in the gas product (18). Furthermore, studies have recently been conducted (20) with a wide variety of catalysts in a fixed-bed reactor to determine the roles of acidity, basicity, and shape selectivity of the catalyst on the conversion of canola oil to various products.

Apart from the catalyst, operating conditions, such as space velocity, reaction temperature and whether or not the oil is cofed with steam, also affect conversion and product distribution (12–19,21,22). These studies showed that an increase in temperature and a decrease in space velocity resulted in an increase in total gas, methane, aromatic, and C_2–C_4 olefin hydrocarbon production, as well as in a decrease in the yields of aliphatic hydrocarbons and coke. Also, the effect of co-feeding canola oil with steam increases the C_2–C_4 olefin hydrocarbon yield. Thus, the literature indicates that information from different sources concerning the effects of various operating conditions on the product distribution is consistent. All these studies were carried out in a fixed-bed reactor.

However, canola oil (or any bio-crude) is a complex feed material, and its conversion to various products involves a complex set of reaction steps (4,17,19). As such, both the feed-catalyst contacting pattern and the duration of contact (i.e., feed-catalyst contacting time) in the reactor are certain to have a tremendous effect on product distribution. Some products of interest obtained from canola oil conversion are: $\geq C_6$ aliphatic hydrocarbons (where $\geq C_6$ means six or more carbon atoms per molecule), $\geq C_6$ aromatic hydrocarbons, C_2–C_4 olefins, and C_4 and C_5 hydrocarbons. It is therefore highly desirable to know how their distribution is affected by the feed-catalyst contacting pattern and duration of contact.

Almost all studies reported in the literature on catalytic conversion of canola oil have been performed in fixed-bed reactors. However, it is well known that the fluidized-bed reactor configuration can offer additional operational advantages, such as catalyst regeneration, which is desirable for the continuous upgrading preferred for industrial operations (23–26). It was therefore decided to carry out a performance evaluation study of various cracking catalysts (namely HZSM-5, silica-alumina, and HS-Mix) for the conversion of canola oil in a fluidized-bed reactor. The results obtained from these studies are presented in this paper.

EXPERIMENTAL PROCEDURES

Canola oil. The canola oil feed material used in this study was obtained from CSP Foods (Saskatoon, Canada). It consisted mainly of unsaturated triglycerides with an average molecular formula of $C_{57}H_{104}O_6$. According to Ackman (27), the fatty acid moieties present in canola oil and their distribution are as follows: 60 mass% oleic acid (18:1), 20% linoleic acid (18:2), 10% linolenic acid (18:3), 2% stearic acid (18:0), 4% palmitic acid (16:0), and small amounts of eicosenic acid (20:0) and erucic acid (22:1) that total close to 4 mass%. The first and second numbers in parentheses refer respectively to the numbers of carbon atoms and C=C bonds per molecule of the acid.

Catalyst selection. The cracking catalysts used were HZSM-5, silica-alumina, and HS-Mix (a physical mixture of 20 mass% HZSM-5 and 80 mass% silica-alumina). They were selected based on previous studies (12–16) in a fixed-bed reactor, which showed that the product distributions obtained with these three catalysts were widely different.

Catalyst preparation. HZSM-5 was prepared according to the procedure reported in the literature (13,14,28), whereas silica-alumina catalyst was obtained from Union Carbide (Danbury, CT) and was activated prior to its use for experimental runs. Catalyst activation was achieved by steam treatment of the catalyst at 630°C for 2 h. Each of the above catalysts was ground and sieved to obtain a particle size range from 104 to 150 μm. HS-Mix catalyst was obtained by physically mixing HZSM-5 catalyst with the activated silica-alumina catalyst in the mass ratio of 1:4. Both catalysts were in the particle size range of 104–150 μm.

Catalysts characteristics. All three catalysts were thoroughly characterized by powder X-ray diffraction (XRD), nitrogen adsorption, temperature-programmed desorption (TPD) of ammonia, Fourier transform infrared (FTIR) of pyridine-adsorbed samples, and solid-state nuclear magnetic resonance (NMR) techniques to determine phase composition, surface area and acidity of the catalysts. HZSM-5 catalyst is known (28) to contain mostly micropores, whereas silica-alumina is reported (13,14) to contain mostly mesopores. Thus, the surface area measured for HZSM-5 represents mostly the inner microporous channel area, while that for silica-alumina represents the Brunauer-Emmett-Teller (BET) surface area generated mostly by the mesopores. The micropore surface area of HZSM-5 was measured by using the Dubinin-Astakhov equation, whereas the BET surface area of silica-alumina was measured by the BET equation (29). Also, the median pore size of HZSM-5 catalyst was estimated with the Hovarth-Kawazoe equation, whereas the average pore size of silica-alumina catalyst was estimated by using the Barrett-Joyner-Halenda (BJH) equation (29).

A summary of the characteristics of the three catalysts is given in Table 1. XRD results, together with surface area and porosimetry analyses, confirmed that HZSM-5 was crystalline and had a uniform pore structure with an average pore size of 0.54 nm. On the other hand, silica-alumina is an amorphous catalyst with an average pore size of 3.15 nm. Also, TPD of NH_3, solid state NMR and FTIR results showed that HZSM-5 contained mostly strong Bronsted acid sites, whereas silica-alumina contained Lewis acid sites. The acid site density given in Table 1 for each catalyst is expressed in terms of the ratio of the total area of TPD of NH_3 peaks to the BET surface area (i.e., mm^2/m^2). In the literature, the acid site density for HZSM-5 and silica-alumina has been expressed either in similar units (i.e., mm^2/m^2) (15,17) or in $mmol/m^2$ (30). Although the latter

TABLE 1
Summary of the Characteristics of the Catalysts

	Characteristics						
Catalyst	Type of acidity[a]	Si/Al ratio	Strength and density[b] (mm^2/m^2) of acid sites	Pore structure	Pore size (nm)	Surface area (m^2/g)	Shape selectivity
HZSM-5	Mostly B	56	Strong (95)	Uniform and crystalline	0.54	329	Very high
HS-Mix	B and L	11.8	Moderate (55)	Mixture of crystalline and amorphous phases	2.63	322	Low
Silica-alumina	B and L	0.79	Moderate (45)	Amorphous	3.15	320	None

[a] B = Bronsted acid sites; L = Lewis acid sites.
[b] Measured by temperature-programmed desorption (TPD) of ammonia.

expression gives the acid site density in absolute terms, we decided to use mm^2/m^2 as a convenient and accurate method to evaluate the relative strengths of the three catalysts. Table 1 shows that the acid site density for HZSM-5 is larger than that for silica-alumina. The acid site density for HS-Mix was in between that of HZSM-5 and silica-alumina (13,14,17,18).

Experimental setup. Figure 1 shows the schematic diagram of the fluidized-bed reactor used for performance evaluation of the catalysts. The reactor consisted of a top cylindrical section (25.4 mm i.d. and 170 overall length), which tapered into a bottom cylindrical section (6.3 mm i.d. and 250 mm length). The vertical height of the tapered section was 10 mm. All reactor components were made of stainless steel (SS 316). The reactor was equipped with a distributor of circular cross-section (25.4 mm diameter and size of openings ≈100 μm), which was located at a vertical distance of 150 mm from the top flange. The reactor was also equipped with a feed inlet tube and a products outlet tube as shown in Figure 1. The reactor did not contain a cyclone separator. However, to minimize catalyst carry-over, the reactor was provided with a large free board section.

The reactor was placed in an electrically heated furnace whose temperature was controlled by a Series SR22 microprocessor-based auto-tuning PID temperature controller (supplied by Shimaden Co. Ltd., Tokyo, Japan) and a K-type thermocouple inserted into the furnace. A separate thermocouple was used to monitor the temperature of the fluidized catalyst bed (Fig. 1). The thermocouple was placed at 24 mm above the static bed height. When the catalyst was fluidized, the thermocouple was at the center of the fluidized bed. This arrangement was capable of ensuring an accuracy of ±2°C for the catalyst bed temperature. The fluidizing gas (argon) entered the reactor from the bottom.

Experimental procedure. Performance evaluation of the catalysts was carried out at atmospheric pressure at temperatures in the range of 400–500°C. This temperature range was selected based on previous studies in a fixed-bed reactor

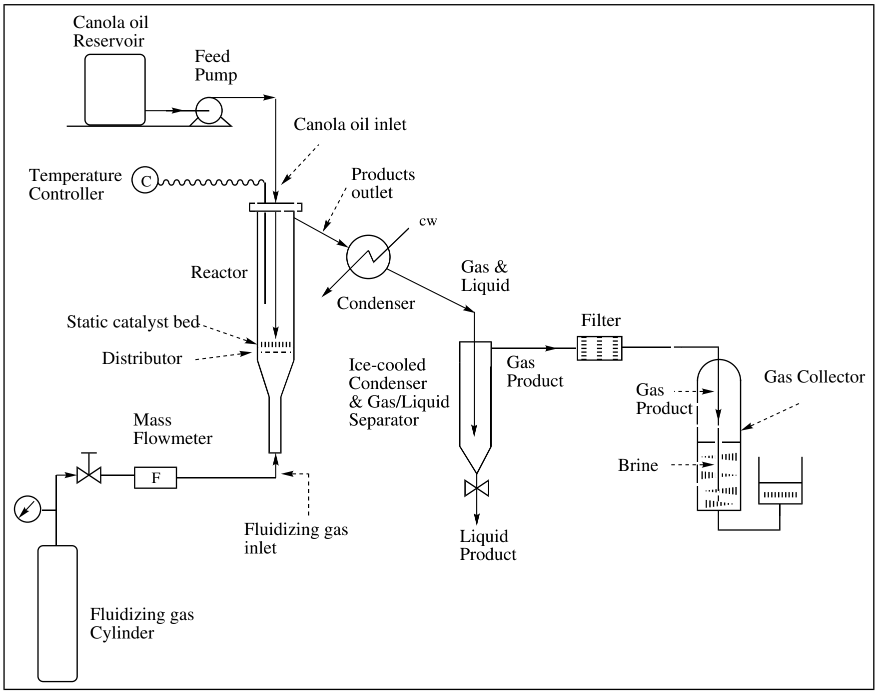

FIG. 1. Schematic diagram of the fluidized-bed reactor experimental set-up.

(12–15,17,18), which showed that various products of interest were obtained within this temperature range.

The minimum fluidizing gas velocity, determined experimentally, was 0.37 m/min at standard temperature and pressure (STP). The actual velocities used for the experimental runs were 0.37, 0.48, and 0.58 m/min at STP. The corresponding fluidizing gas flow rates were 175, 225, and 275 mL/min at STP. Canola oil flow rate was constant for all runs (0.6 g/min), and the feed vapor was assumed to be entrained in the fluidizing gas.

A typical fluidized-bed reactor run was performed as follows: The reactor was loaded by placing 10 g of the desired catalyst on top of the distributor, below which was a plug of glass wool, which provided an additional screen for the catalyst. The reactor was then heated in the flowing argon gas (175 mL/min) to the desired reaction temperature. After the desired temperature was reached, the argon flow was adjusted to achieve the desired fluidizing gas flow rate. Canola oil was then fed to the reactor from the top by an Eldex micrometering pump (Model A-60-S; supplied by Terochem Laboratories Ltd., Edmonton, Canada) at the rate of 0.6 g/min. The product mixture from the reactor was cooled in a chilled water-cooled condenser. The liquid product was separated from the gas product in a gas–liquid separator/ice trap, which also served as liquid collector. The gas product passed on to the gas collector where it was trapped over brine. Each experimental run lasted 20 min.

Analysis of the products. The liquid product was distilled at 200°C and a vacuum of 172 Pa in a Buchi GKR-50 (Buchi Company, Flawil, Switzerland) distillation unit. The distillate obtained was referred to as OLP, and the residue was termed residual oil. The products collected for each run were: gas, OLP, residual oil, and coke. Details concerning their collection are given elsewhere (13,14,19). The chemical composition of the gas and OLP fractions were determined with a Carle gas chromatograph (Model 500; Carle Instruments Inc., Anaheim, CA), equipped with a flame ionization detector (FID) and a thermal conductivity detector (TCD). Usually, the OLP fraction contains a wide variety of components (hydrocarbons with isomers and various functional groups). Therefore, gas chromatograph–mass spectrometer (GC–MS) analysis in conjunction with the use of known pure compounds and calibration mixtures (PolyScience Corp., Niles, IL) was necessary to establish the identity of the components in OLP. GC–MS analysis was performed in a VG Analytical 70VS extended magnet mass spectrometer (VG Analytical 8000, Manchester, United Kingdom), attached to a VG 800 series GC (VG Analytical 8000). The components were identified by their mass spectra. The VG 800 GC (used for GC–MS analysis) was equipped with the same set of columns and was operated under the same oven temperature program as the Carle GC (used for purely GC analysis). Details of these analysis procedures are given elsewhere (13,14,19). The entire reaction procedure was repeated a number of times for some runs to check reproducibility. The error was less than ±3 mass% in terms of both canola oil conversion and yields of products.

RESULTS AND DISCUSSION

Effects of operating variables on canola oil conversion. The mass balances, canola oil conversions, and yields of various products obtained for the catalytic conversion of canola oil in a fluidized-bed reactor with HZSM-5, HS-Mix, and silica-alumina catalysts are given, respectively, in Tables 2, 3, and 4 as a function of reaction temperature and fluidizing gas velocity. These tables show that there are dramatic changes in the conversion and production distribution of canola oil due to the type of catalyst used and to changes in operating variables. Catalysis literature indicates that such changes are due to the effects of both the characteristics of the catalyst and the operating variables on the reaction mechanism. In an earlier study (17), a reaction scheme was proposed to show the reaction sequence for the formation of various products from canola oil conversion. This sequence is given as follows:

$$\text{canola oil} \rightarrow \text{long-chain } C_xH_y + \text{long-chain oxygenated } C_xH_y \text{ (thermal)} \qquad [1]$$

$$\text{long-chain oxygenated } C_xH_y \rightarrow \text{long-chain } C_xH_y + H_2O + CO_2 + CO \text{ (thermal + catalytic)} \qquad [2]$$

TABLE 2
Mass Balances and Yields of Gaseous Products for HZSM-5 Catalyst

Temperature (°C)	400			450	500	
Fluidizing gas velocity (m/min)	0.37	0.48	0.58	0.48	0.48	0.58
Mass balance (wt% of canola oil fed)						
Gas	28	30	32	42	60	62
OLP	44	35	29	32	20	13
Residual oil	7	12	16	7	2	5
Coke	5	5	4	4	2	4
Unaccounted	16	18	19	15	16	16
Total	100	100	100	100	100	100
Conversion	93	88	84	93	98	95
Yields of gaseous products (wt% of canola oil fed)						
Methane	0.1	0.1	0	0.1	0.4	0.6
Ethylene	2.0	1.5	1.6	0.2	6.0	6.8
Ethane	0.3	0.3	0.1	3.4	0.6	0.6
Propylene	4.5	4.2	5.1	8.0	12.6	18.6
Propane	4.5	5.1	3.8	2.9	1.8	2.4
n-Butane	2.5	2.4	2.9	4.2	6.0	7.4
iso-Butane	2.5	2.1	1.6	2.9	3	0.6
iso-Butylene	2.8	3.3	3.2	4.2	4.8	4.3
1- and 2-Butenes	0.5	1.2	0.7	4.0	2.4	2.5
C_5 Hydrocarbons	8.3	7.2	9.7	7.6	16.8	12.4
CO and CO_2	3.1	2.6	3.3	4.5	5.6	5.8
Total	28	30	32	42	60	62
C_2–C_4 Olefins	9.8	10.2	10.6	16.4	25.8	32.2

TABLE 3
Mass Balances and Yields of Gaseous Products for HS-Mix Catalyst

Temperature (°C)	400	450	500
Fluidizing gas velocity (m/min)	0.48	0.48	0.48
Mass balance (wt% of canola oil fed)			
Gas	22	39	52
OLP	28	32	20
Residual oil	15	12	10
Coke	15	6	5
Unaccounted	20	11	13
Total	100	100	100
Conversion	85	88	90
Yields of gaseous products (wt% of canola oil fed)			
Methane	0	0.3	1.0
Ethylene	0.9	2.0	3.6
Ethane	0.1	0.4	1.0
Propylene	3.5	9.4	15.1
Propane	1.3	2.0	2.6
n-Butane	1.3	3.1	6.8
iso-Butane	4.0	3.9	1.0
iso-Butylene	2.0	3.9	5.7
1- and 2-Butenes	0	0	0
C_5 Hydrocarbons	6.9	10.9	11.6
CO and CO_2	2.0	3.1	3.6
Total	22	39	52
C_2–C_4 Olefins	6.4	15.2	24.4

TABLE 4
Mass Balances and Yields of Gaseous Products for Silica-Alumina Catalyst

Temperature (°C)	400		450	500	
Fluidizing gas velocity (m/min)	0.37	0.48	0.48	0.48	0.58
Mass balance (wt% of canola oil fed)					
Gas	18	20	35	55	57
OLP	30	22	29	17	14
Residual oil	15	19	14	9	10
Coke	16	18	5	5	5
Unaccounted	21	21	17	14	14
Total	100	100	100	100	100
Conversion	85	81	86	91	90
Yields of gaseous products (wt% of canola oil fed)					
Methane	0.2	0	0.4	1.6	1.7
Ethylene	0.4	0.2	0.7	1.6	1.7
Ethane	0.2	0	0.7	1.1	1.1
Propylene	2.5	1.6	4.2	6.6	7.4
Propane	0.7	0.6	1.4	3.3	2.3
n-Butane	0.7	0.4	1.8	2.8	3.4
iso-Butane	2.2	2.2	2.5	5.0	5.1
iso-Butylene	1.3	1.2	2.1	5.0	4.0
1- and 2-Butenes	0.7	0	0.7	0.6	1.7
C_5 Hydrocarbons	6.8	10.2	16.9	22.3	22.3
CO and CO_2	2.3	3.6	3.6	5.1	6.3
Total	18	20	35	55	57
C_2–C_4 Olefins	4.9	3.0	7.7	13.8	14.8

$$\begin{gathered}\text{long-chain } C_xH_y \rightarrow \text{paraffins} + \text{olefins} \\ \text{(short- and long-chain)} \\ \text{(thermal + catalytic)}\end{gathered} \qquad [3]$$

$$\text{short-chain olefins} \rightarrow C_2\text{–}C_{10} \text{ olefins (catalytic)} \qquad [4]$$

$$\begin{gathered}C_2\text{–}C_{10} \text{ olefins} \leftrightarrow \text{aliphatic } C_xH_y + \\ \text{aromatic } C_xH_y \text{ (catalytic)}\end{gathered} \qquad [5]$$

$$\text{canola oil} \rightarrow \text{coke (thermal)} \qquad [6]$$

$$n(\text{aromatic } C_xH_y) \rightarrow \text{coke (catalytic)} \qquad [7]$$

Here, "long-chain" is used as a qualifier for hydrocarbons and oxygenated hydrocarbons that contain many carbon atoms per molecule, while "short chain" is used as a qualifier for hydrocarbons and oxygenated hydrocarbons that contain few carbon atoms per molecule. Furthermore, C_xH_y stands for hydrocarbons.

In this scheme, Equations 1 and 2 involve the primary cracking of canola oil molecules to give a mixture of long-chain hydrocarbons and long-chain oxygenated hydrocarbons. This mixture is regarded as "residual oil," which may undergo further deoxygenation (Eq. 2) and/or secondary cracking (Eq. 3) to give olefins and paraffins. The short-chain olefins oligomerize (Eq. 4) to yield olefins in the C_2–C_{10} range. Aromatic as well as cyclic aliphatic hydrocarbons are eventually produced (Eq. 5) as a result of cyclization and aromatization reactions of the C_2–C_{10} olefins. Coke is formed either due to polycondensation of canola oil molecules (Eq. 6) or polymerization of large aromatic hydrocarbon molecules (Eq. 7). This sequence also indicates that steps 1 and 6 are predominantly thermal, whereas steps 4, 5, and 7 are predominantly catalytic (but they are also strongly enhanced by temperature). Step 2 involves both thermal and catalytic reactions, which may occur to comparable extents. Furthermore, gas is obtained in steps 2 and 3, and part of this gas is used up in steps 4 and 5. It is implied that the straight and branched-chain aliphatic hydrocarbon components of OLP are obtained mainly in step 3, while the cyclic aliphatic, mono-aromatic and poly-aromatic hydrocarbon components of OLP are obtained mainly in step 5. The reaction scheme can be used to develop an understanding of the effect of various operating variables on the product distribution obtained in a fluidized-bed reactor.

Effects of reaction temperature. Tables 2, 3, and 4 show that canola oil conversions for all three catalysts were high (in the range of 79–98 wt%). Canola oil conversion and the total amount of gas produced increased with reaction temperature, as expected. On the other hand, Figures 2 and 3 show that there were differences in the response of the yields of some components in the gas and OLP fractions to changes in reaction temperature. For example, Figure 2 shows that the yields of C_4 and C_5 hydrocarbons and of C_2–C_4 olefins (all components of the gas product) increased with reaction temperature. These results are consistent with an increase in the

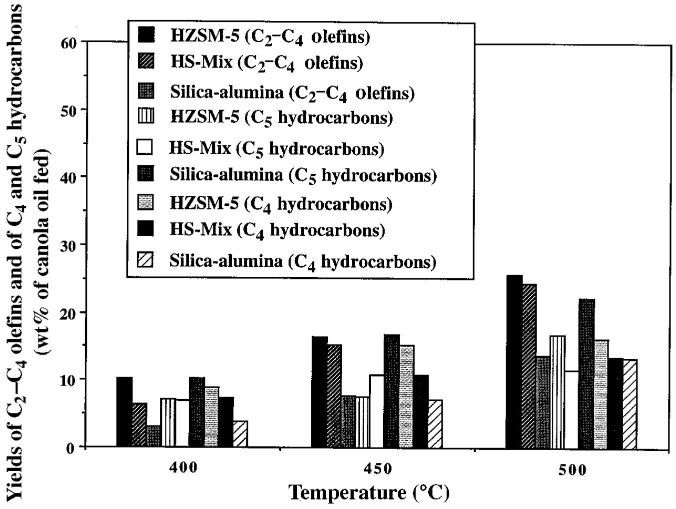

FIG. 2. Yields of C_2–C_4 olefins and C_4 and C_5 hydrocarbons as a function of temperature and type of catalyst.

extent of both primary and secondary cracking of canola oil (Eqs. 1–3) with temperature (13,14,17,19), which results in an increase in the gas yield.

In contrast, Figure 3 shows that the yield of aromatic hydrocarbons increased with temperature, whereas that of $\geq C_6$ aliphatic hydrocarbons decreased with temperature. This can be explained as follows: Equation 5 indicates that both aromatic and cyclic aliphatic hydrocarbons are formed from C_2–C_{10} olefins. It is well known (17) that the formation of cyclic aliphatic hydrocarbons is an intermediate step in the formation of aromatic hydrocarbons from C_2–C_{10} olefins. It is also known that both the extents of cyclization (to form cyclic aliphatic hydrocarbons) and aromatization (to form aromatic hydrocarbons) increase with temperature. However, reaction engineering literature shows that an increase in temperature is certain to be more beneficial for the formation of terminal products (which are aromatic hydrocarbons for this particular reaction route) than intermediate products (which are cyclic aliphatic hydrocarbons). The implication is that the net formation of aromatic hydrocarbons increases at a faster rate with temperature than the net formation of aliphatic hydrocarbons (19,20).

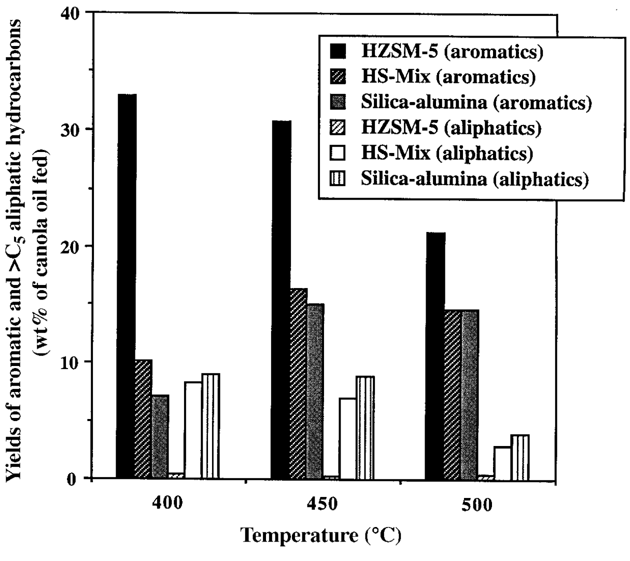

FIG. 3. Yields of aromatic and aliphatic hydrocarbons as a function of temperature and type of catalyst.

Tables 2, 3, and 4 also show that the yield of coke decreased as the cracking temperature was increased. This can be explained because an increase in temperature facilitates coke gasification and results in a net decrease in the amount of coke formed (13,14).

Effect of type of catalyst on canola oil conversion. Tables 2–5 show that, under similar temperatures and fluidizing gas velocities, canola oil conversions for the three catalysts decreased in the order: HZSM-5 > HS-Mix > silica-alumina. A comparison of Tables 2–4 with Table 1 shows that the activity order exhibited by the catalysts (Tables 2–4) follows the same decreasing order as their acid site density, crystallinity, and shape selectivity (Table 1). As indicated in the reaction sequence (Eqs. 1–7), the initial reaction in canola oil conversion is thermal cracking of the triglyceride molecules (step 1). Subsequently, the cracked molecules undergo various secondary reactions on the surface or within the pores of the catalysts. The literature (17) shows that these secondary reactions, and consequently the final product distribution, strongly depend on the characteristics of the catalysts. For example, some of the forward reaction steps given in the reaction sequence (namely, Eqs. 2–5) are catalyzed by Bronsted acid centers. This implies that the greater the Bronsted acid site density, the greater the shift in equilibrium in favor of the forward reactions, and consequently, the greater the conversion. This is responsible for the increase in canola oil conversion with acid site density and hence the activity order of the catalysts.

Effect of type of catalyst on gas and OLP yields. The yields of gas and OLP for fluidized-bed reactor test runs increased in the same order as canola oil conversion (Fig. 4, Tables 2–4). This implies that both gas and OLP (Fig. 4) increased in the same order as acid site density (Table 1), although the increase for OLP was insignificant at the higher temperatures. These trends are in contrast to those obtained in our earlier work in a fixed-bed reactor (13,14,17) where an increase in the Bronsted acid site density in the catalyst resulted in an increase in OLP yield but a decrease in gas yield. These results are explained below.

It is implied in the reaction sequence that gas as well as straight or branched-chain aliphatic hydrocarbon and oxygenated hydrocarbon components in OLP are formed in step 3. Apart from these, other components of OLP (namely, olefinic, cyclic, and aromatic hydrocarbons) are formed after steps 2 and 3 (the gas formation steps) by the reactions of C_2–C_5 olefins and dienes in steps 4 and 5. The consequence of these reactions can be seen clearly in Figure 3 (for aromatic hydrocarbon components of OLP) where the relative fraction

TABLE 5
Comparison Between the Performance of Catalysts in Fluidized- and Fixed-Bed Reactors

Temperature (°C)	400				450				500			
Catalyst used	HZSM-5		Silica-alumina		HZSM-5		Silica-alumina		HZSM-5		Silica-alumina	
Reactor type[a]	1	2	1	2	1	2	1	2	1	2	1	2
Mass balances (wt% of canola oil fed)												
Gas	25	30	11	20	34	42	29	35	50	60	45	55
OLP	63	35	40	22	56	32	51	29	41	20	42	17
Residual oil	3	12	7	19	1	7	4	14	0	2	1	9
Coke	3	5	36	18	4	4	13	5	5	2	10	5
UN[b]	6	18	6	21	5	15	3	17	4	16	2	14
Total	100	100	100	100	100	100	100	100	100	100	100	100
Selectivities for formation of gas (OLP and C_2–C_4 olefins)												
G/O ratio[c]	0.4	0.86	0.28	0.91	0.61	1.31	0.57	1.21	1.22	3.0	1.07	3.24
C_2–C_4 olefins (wt% of gas)	16	33	25	15	29	39	28	22	34	43	29	25
Concentrations of various components of OLP (wt% of OLP)												
Ar H/C[d]	82	87	28	29	88	87	34	44	96	90	53	63
Al H/C[e]	1.6	1.0	30	37	0.8	0.6	22	26	0.3	2	14	17
Others	16.4	12	42	34	11.2	12.4	44	30	3.7	8	33	20

[a] 1, Fixed-bed reactor operation (weight hourly space velocity = 1.8^{-1}); 2, fluidized-bed reactor operation (fluidizing gas velocity = 0.48 m/min).
[b] UN, unaccounted fraction.
[c] G/O, gas product/OLP weight ratio.
[d] Ar H/C, aromatic hydrocarbons.
[e] Al H/C, aliphatic hydrocarbons.

of aromatic hydrocarbons increased with the acid site density of the catalyst. Therefore, because the gas and OLP fractions are not formed during the same reaction step, their yields will depend strongly on the time of contact between the feed/reaction mixture and catalyst. This time of contact is longer in the fixed-bed reactor than in the fluidized-bed reactor. Our earlier results for the fixed-bed reactor (13,14) showed that there is sufficient contact time for both gas formation steps (steps 2 and 3) as well as the subsequent acid site-catalyzed reactions, involving the consumption of C_2–C_5 olefins in the gas product (steps 4 and 5), to occur. Hence, the increase in OLP yield and the corresponding decrease in gas yield occur with an increase in acid site density for the fixed-bed reactor.

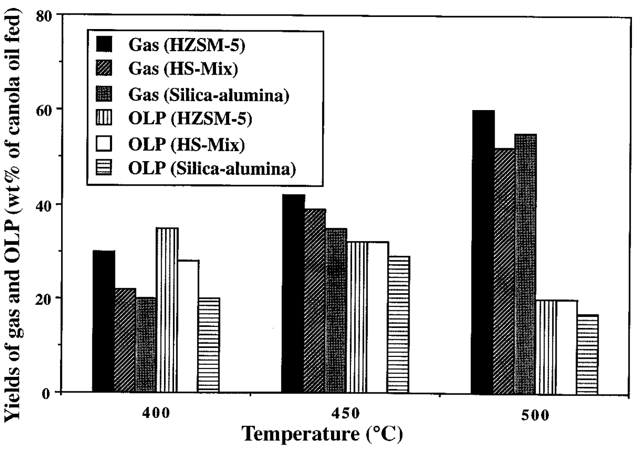

FIG. 4. Yields of gas and OLP as a function of temperature and type of catalyst.

On the other hand, the present results indicate that, while the contact times used in the fluidized-bed reactor were sufficient for gas formation (as in steps 2 and 3) as well as OLP formation (as in step 3) to occur, it was barely sufficient for the formation of OLP components obtained by the reactions involving C_2–C_5 olefins, as in steps 4 and 5. Thus, even though an increase in catalyst acid site density alone can enhance the formation of additional OLP from C_2–C_5 olefins, as in steps 4 and 5, the rather short average contact time in the fluidized-bed reactor appears to permit only small amounts of these olefins to be depleted.

Furthermore, Figure 4 shows a substantial increase in the gas yield and only a marginal increase in the OLP yield with acid site density at the two higher reaction temperatures. This can be explained because reactions 2 and 3 (for the formation of gas) are known (19) to be enhanced by temperature to a greater extent than reaction steps 4 and 5 (for the formation of OLP).

Combined effect of catalyst acidity and temperature on OLP yield. Figure 5 shows the yields of OLP for HZSM-5, HS-Mix, and silica-alumina catalysts for runs carried out in the fluidized-bed reactor at various reaction temperatures. The figure shows that a maximum exists at 450°C in OLP yield for HS-Mix and silica-alumina catalysts. On the other hand, for HZSM-5 catalyst there was a monotonic decrease in OLP yield with an increase in temperature. These results can be explained as follows: The literature (13,14,17,20) shows that the formation of OLP according to reactions 4 and 5 is influenced by three major factors: (i) acid site density of the catalyst, (ii) feed-catalyst contact time, and (iii) reaction temperature. As shown in Table 1, the acid sites present in HS-Mix and silica-alumina are weak compared to those in HZSM-5. Thus, for HS-Mix and silica-alumina catalysts (containing weak acid sites), the feed-catalyst contact time becomes irrelevant for acid-catalyzed reactions 4 and 5. The result is that temperature becomes the major factor for OLP formation. Consequently, at 400°C (low temperature), there is limited cracking of residual oil (step 3), resulting in the production of only small amounts of both gas and OLP while a large amount of residual oil still remains uncracked. In contrast, there is severe cracking of residual oil at 500°C, resulting in the conversion of a substantial portion of the residual oil; also, most of the cracked products at this temperature end up in the gas product instead of OLP. The result is the production of small amounts of OLP at both 400 and 500°C. Cracking of residual oil at 450°C is more severe than at 400°C. However, unlike at 500°C, a large portion of the product ends up as OLP. This is responsible for the larger yield of OLP at 450°C than those obtained at either 400 or 500°C, hence the maximum yield of OLP at 450°C for HS-MIX and silica-alumina.

Figure 5 shows that the main difference between the OLP yield-temperature trends for HS-Mix and silica-alumina and that for HZSM-5 is the unexpected high OLP yield for HZSM-5 at 400°C. This can be attributed to the high acid site density of HZSM-5 in conjunction with the use of a fluidized-bed reactor for canola oil conversion. Unlike silica-alumina and HS-Mix catalysts (containing relatively low acid site densities), the high acid site density in HZSM-5 catalyst promotes extensive cracking of residual oil. This is confirmed by the higher canola oil conversion obtained for HZSM-5 catalyst than for either HS-Mix or silica-alumina catalyst. Usually, a high degree of cracking results in the formation of a large amount of gas product (instead of OLP) if the reactor can provide a long feed-catalyst contact time that permits extensive cracking of individual molecules of residual oil. This can be achieved with a fixed-bed reactor, even for cracking at 400°C. However, because of the relatively short feed-catalyst contact time possible in the fluidized-bed reactor, the severity of cracking is reduced and, at 400°C, a substantial portion of the cracked product ends up in the OLP fraction. This is responsible for the high yield of OLP at 400°C for the run with HZSM-5 catalyst in a fluidized-bed reactor.

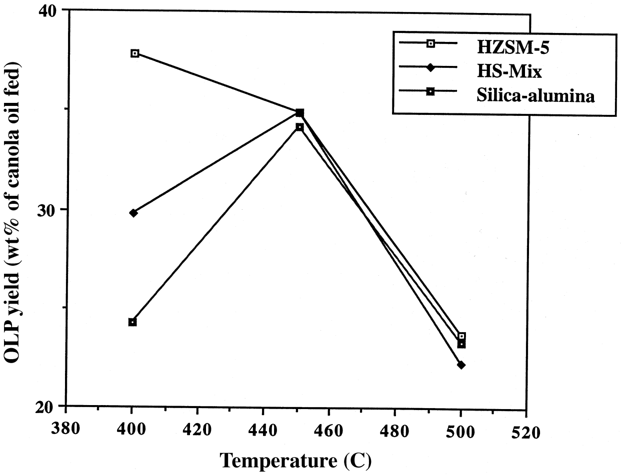

FIG. 5. Effect of the type of catalyst on the variation of OLP yield with temperature.

Coke formation and composition of the gas product. Tables 2, 3, and 4 show, respectively, the yields of coke obtained for HZSM-5, HS-Mix, and silica-alumina catalysts. These tables show that coke formation increased in the order: HZSM-5 < HS-Mix < silica-alumina. This is consistent with results obtained in our earlier work with a fixed-bed reactor (13,14), which showed that coke formation decreased with an increase in Bronsted acid site density. As was shown in these studies, a high catalyst acid site density enhances coke gasification.

Usually, the components of interest in the gas product are the C_2–C_4 olefins and C_4 and C_5 hydrocarbons. Figure 2 shows that, for runs in a fluidized-bed reactor, there were drastic variations in the yields of these components with the type of catalyst used. For example, this figure shows that the yields of C_4 hydrocarbons and C_2–C_4 olefins decreased in the order HZSM-5 > HS-Mix > silica-alumina (decreasing catalyst acid site density), whereas a reverse trend was observed for C_5 hydrocarbons. The results for C_5 hydrocarbons are consistent with those in the literature (13,14,19,20), whereas results for C_4 hydrocarbons and C_2–C_4 olefins are in contrast to those obtained in a fixed-bed reactor (13,14,20) where the yields decreased in the order: silica-alumina > HS-Mix > HZSM-5. For C_2–C_4 olefins, the literature (13,14) shows that the higher the acid site density, the greater the extent of cracking of residual oil to produce olefins (step 3). However, the short feed-catalyst contact time, which is characteristic of the fluidized-bed reactor, does not permit a significant portion of these olefins to be converted to OLP according to steps 4 and 5, hence, the increase in the yield of C_2–C_4 olefins with acid site density. For the relatively low molecular weight C_4 hydrocarbon gases, it has been shown (19,20) that their formation from canola oil depends on both the acid site density and the feed-catalyst contact time. Usually, a long contact time in conjunction with a high acid site density should result in the formation of light hydrocarbon gases (carbon number in the range 1–3). However, the short feed-catalyst contact time available for fluidized-bed reactor operation is such that secondary cracking for C_4 hydrocarbon formation becomes a function mainly of catalyst acidity, hence, the trend for the yield of C_4 hydrocarbons with respect to the type of catalyst.

Effect of fluidizing gas velocity on canola oil conversion. Table 2 shows the typical variations of canola oil conversion and the yield of residual oil for the catalytic cracking of canola oil at 400°C for HZSM-5 catalyst in a fluidized-bed reactor. Canola oil conversion was higher for runs conducted at low fluidizing gas velocity than for those at high fluidizing gas velocity. As is well known, the effect of increasing the gas velocity for fluidized-bed reactor operation is to decrease the contact time between the feed and the catalyst. Usually, this results in a decrease in the conversion of the feed, as shown in Table 2.

Effect of fluidizing gas velocity on gas and OLP yields. Table 2 also shows variations of yields of total gas, OLP, and coke for HZSM-5 catalyst in a fluidized-bed reactor at 400°C. An increase in fluidizing gas velocity results in an increase in the gas yield and a decrease in OLP yield. These trends are contrary to the results obtained for runs in a fixed-bed reactor for an increase in space velocity (13,14). These results for both gas and OLP can be explained on the basis of the reaction sequence given in Equations 1–7. This sequence indicates that the reaction steps that result in the formation of gas products (Eqs. 2 and 3) occur much earlier than those that lead to subsequent consumption of the gas produced to form OLP (Eqs. 4 and 5). Thus, within the range of fluidizing gas velocities used, an increase in fluidizing gas velocity does not affect gas production whereas it adversely affects subsequent conversion of gas to OLP. Usually, this should result in a corresponding decrease in the yield of OLP with an increase in fluidizing gas velocity. Our results (Table 2) show that there was a decrease in the yield of OLP with an increase in fluidizing gas velocity.

Effect of fluidizing gas velocity on residual oil yield. Table 2 shows that, for runs in the fluidized-bed reactor, not only was the amount of residual oil larger, but it also contained concentrations of oxygenated hydrocarbons, which increased as the fluidizing gas velocity increased. For example, GC–MS analysis showed qualitatively that the amounts of stearic and palmitic acids were larger for runs at 0.58 m/min (at STP) than for those at 0.37 m/min (at STP). These results are consistent with those reported in the literature and can be explained as follows: Long-chain oxygenated hydrocarbons are products of the initial decomposition of canola oil (step 1). As shown in the reaction scheme, subsequent reactions are decarboxylation and decarbonylation of these oxygenated hydrocarbon products (step 2) as well as C-C bond cleavage of the resulting heavy hydrocarbons (Eq. 3). This means that the amount of long-chain oxygenated hydrocarbons produced depends on the average feed-catalyst contact time used for the reaction. As was mentioned earlier, a low fluidizing gas velocity is favorable for subsequent decomposition of an intermediate product (heavy oxygenated hydrocarbons in this case), whereas a high fluidizing gas velocity is not. The consequence is the presence of large amounts of heavy oxygenated hydrocarbons for high fluidizing gas velocity.

Comparison of the performance of the catalysts in a fluidized-bed reactor with that in a fixed-bed reactor. A comparison between the performance of HZSM-5 and silica-alumina catalysts in a fluidized-bed reactor and in a fixed-bed reactor [obtained from our earlier work (13,14)] is given in Table 5. The mass balances shown in Table 5 indicate that, generally, there were relatively more losses in fluidized-bed reactor operations than in the fixed-bed reactor. These losses are referred to as “unaccounted fraction.” The slightly larger losses in fluidized-bed reactor operation show that there was some entrainment of catalyst particles in the runs. In such cases, the amounts of coke and residual oil carried along with the catalyst particles were not included in the mass balance. This accounts for the larger unaccounted fractions shown for the fluidized-bed reactor.

Gas and OLP yields. Table 5 shows that, for similar catalysts at corresponding temperatures, canola oil conversions and yields of gas and OLP fractions for runs in a fluidized-bed reactor were lower than those obtained for runs in a fixed-bed reactor. As discussed earlier, these lower conversions and yields can be attributed principally to the short average feed-catalyst contact times in the fluidized-bed reactor compared to those in the fixed-bed reactor.

Table 5 also shows that, for corresponding temperatures, the ratios of the yields of gas and OLP were higher for runs in the fluidized-bed reactor than for those in a fixed-bed reactor. This higher gas/OLP ratio implies that the net rate of formation of gas is higher in the fluidized-bed reactor than in the fixed-bed reactor, and conversely, that the net rate of formation of OLP is lower in the fluidized-bed reactor than in the fixed-bed reactor. This can be explained from the average contact times employed for the two types of reactors in conjunction with the reaction sequence given in Equations 1–7. These show that, in the fluidized-bed reactor, the short average contact times were sufficient for reactions that led to the formation of gas products (Eqs. 2 and 3) to take place but not sufficient for the subsequent reactions of the gas to form OLP (Eqs. 4 and 5). This is responsible for the high gas/OLP ratios for operations in the fluidized-bed reactor. In contrast, the long average contact time used in the fixed-bed reactor was sufficient for both types of reactions (reactions 2 and 3, and reactions 4 and 5) to take place. Consequently, large amounts of OLP were formed at the expense of the gas products for runs in the fixed-bed reactor.

Selectivities for the formation of C_2–C_4 olefins, C_5 hydrocarbons, iso-*butane and* iso-*butylene*. Table 5 shows that, for HZSM-5 catalyst, the selectivity for the formation of C_2–C_4 olefins was higher for operations in the fluidized-bed reactor than in the fixed-bed reactor. This is consistent with the short average feed-catalyst contact times available in the fluidized-bed reactor and becomes advantageous if C_2–C_4 olefins are the desired products. In contrast, Table 5 shows that, for silica-alumina catalyst, the selectivity for the formation of C_2–C_4 olefins was lower in the fluidized-bed reactor than in the fixed-bed reactor. This can be explained as follows. The acid site density for silica-alumina is low (Table 1). Consequently, cracking of residual oil to produce olefins (step 3) with silica-alumina is due mainly to thermal effects. Cracking according to step 3 requires a long feed-catalyst contact time for silica-alumina catalyst compared with the time required for HZSM-5 catalyst, which has a high acid site density (Table 1). This long contact time can be achieved more readily in a fixed-bed reactor than in a fluidized-bed reactor. Thus, the long contact times for the fixed-bed reactor ensure the production of large amounts of C_2–C_4 olefins. However, the low acid site density of silica-alumina is such that only a small amount of these olefins is depleted for the formation of OLP according to reactions 4 and 5. For fluidized-bed reactor operation, the short contact times are such that not only are small amounts of C_2–C_4 olefins produced (according to reaction 3), but also an insignificant amount of these olefins are depleted for the formation of OLP (according to reactions 4 and 5). The net result is a low selectivity for C_2–C_4 olefins for the silica-alumina catalyst in a fluidized-bed reactor.

For HZSM-5 catalyst, the long feed-catalyst contact times in the fixed-bed reactor, coupled with the high acid site density of the catalyst, are such that the formation (reaction 3) and depletion (reactions 4 and 5) of C_2–C_4 olefins both take place to substantial extent. Thus, a substantial amount of the C_2–C_4 olefins formed is depleted for the formation of OLP (reactions 4 and 5). On the other hand, the short feed-catalyst contact time in the fluidized-bed reactor, coupled with the use of HZSM-5 catalyst (containing strong acid sites), ensures that only the formation of C_2–C_4 olefins (reaction 3) takes place to a substantial extent, mainly on account of the presence of strong acid sites in the catalyst. The contact time in the fluidized-bed reactor is insufficient for the depletion of these olefins according to reactions 4 and 5. This is responsible for the observed high selectivity for C_2–C_4 olefins for HZSM-5 catalysts in the fluidized-bed reactor and a low selectivity for C_2–C_4 olefins in the fixed-bed reactor.

Figure 6 shows the concentrations of C_5 hydrocarbons and of *iso*-butane and *iso*-butylene (branched C_4 hydrocarbons) in the gas product as a function of the type of reactor. This figure shows that the concentrations of C_5 hydrocarbons and of *iso*-butane and *iso*-butylene in the gas product were higher for canola oil conversions in the fluidized-bed reactor than in the fixed-bed reactor. For *iso*-butane and *iso*-butylene, this implies that the degree of isomerization was not only higher, but also that there appears to be no subsequent conversion of these gas-phase *iso*-C_4 hydrocarbons to components in the OLP fraction or other products for runs in the fluidized-bed reactor when compared with those in the fixed-bed reactor. Because there were no significant changes in the yields of these *iso*-C_4 hydrocarbons with changes in fluidizing gas velocity, this suggests that isomerization reactions are favorable with the feed-catalyst contacting pattern that exists in the fluidized-bed reactor. The C_5 hydrocarbons can be explained from the shorter feed-catalyst contact time for fluidized-bed reactor operation than for fixed-bed reactor operation. A short contact time limits the severity of cracking such that most of the C_5 hydrocarbons formed do not undergo further C-C bond scission into smaller molecules.

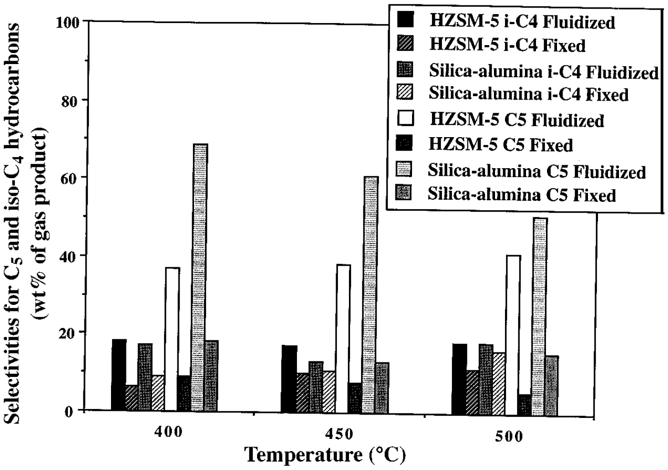

FIG. 6. Comparison between C_5 and *iso*-C_4 hydrocarbons obtained in the fluidized-bed reactor and in the fixed-bed reactor.

Selectivities for the formation of aromatic and aliphatic hydrocarbons. The concentrations of aromatic hydrocarbons in OLP for operations in the two types of reactors with HZSM-5 and silica-alumina catalysts are shown in Table 5. As expected, the concentrations of aromatic hydrocarbons were higher for runs in a fixed-bed reactor than for those in a fluidized-bed reactor at 450 and 500°C, where the concentrations of unidentified products were relatively small. On the other hand, the concentrations of aliphatic hydrocarbons for operations with silica-alumina were higher for runs in the fluidized-bed reactor than for those in the fixed-bed reactor at 500°C, where the concentrations of unidentified products were relatively small. The results at these high temperatures are consistent with the long average contact times that exist in the fixed-bed reactor when compared to those in the fluidized-bed reactor, as well as with the low acid site density of silica-alumina compared to that of HZSM-5. These results further support our assertion that the steps that result in the formation of aliphatic hydrocarbons occur earlier than those for the formation of aromatic hydrocarbons and that aromatization reactions benefit more from an increase in acid site density than aliphatic hydrocarbon formation.

ACKNOWLEDGMENT

The financial support of the Natural Sciences and Engineering Research Council of Canada (NSERC) is gratefully acknowledged.

REFERENCES

1. Campbell, I.M., *Biomass, Catalysts and Liquid Fuels*, Holt, Rinehart and Winston, London, 1983.
2. Parkinson, G., Refining's New Jingle, *Chemical Eng. 99*:35–39 (1992).
3. Baker, E.G., and C.D. Eliott, Catalytic Upgrading of Biomass

Pyrolytic Oils, in *Research in Thermochemical Biomass Conversion*, edited by A.V. Bridgwater, ACS Division of Fuel Chemistry, Elsevier Appl. Sci., London, 1987, pp. 883–895.

4. Boocock, D.G.B., S.K. Konar, A. Mackay, P.T.C. Cheung, and J. Liu, Fuels and Chemicals from Sewage Sludge, *Fuel 71*:1291–1297 (1992).
5. Sharma, R.K., and N.N. Bakhshi, *Catalytic Conversion of Crude Tall Oil to Fuels and Chemicals,* Report of Contract File No. 0582-23283-8-6116, Renewable Energy Branch, Energy, Mines and Resources Canada, Ottawa, Canada, 1989.
6. Adjaye, J.D., and N.N. Bakhshi, Production of Hydrocarbons by Catalytic Upgrading of Fast Pyrolysis Bio-Oil: Part 1. Conversion over Various Catalysts, *Fuel Proc. Tech. 45*:161–183 (1995).
7. Perterson, C.L., H. Haines, and C. Chase, Rapeseed and Safflower Oils as Diesel Fuel, in *Proceedings of the 1st Biomass Conference of the Americas: Energy, Environment, Agriculture and Industry,* Burlington, VT, (NREL, Golden, CO) 1993, pp. 922–927.
8. Craig, W., and E. Coxworth, Conversion of Vegetable Oils to Conventional Liquid Extenders, in *Proceedings of the 6th Canadian Bioenergy R&D Seminar,* edited by C. Granger, Richmond, BC, Canada, Elsevier Appl. Sci., London, Feb. 16–18, 1987, pp. 407–411.
9. Sharma, R.K., and N.N. Bakhshi, Catalytic Conversion of Crude Tall Oil to Fuels and Chemicals over HZSM-5: Effect of Co-Feeding Steam, *Fuel Proc. Tech. 27*:113–130 (1991).
10. Chantal, P., S. Kaliaguine, J.L. Grandmaison, and A. Mahay, Production of Hydrocarbons from Aspen Poplar Pyrolysis Oil over HZSM-5, *Appl. Catal. 10*:317–332 (1984).
11. Sharma, R.K., and N.N. Bakhshi, Catalytic Upgrading of Pyrolysis Oil, *Energy Fuels 7*:306–319 (1993).
12. Prasad, Y.S., N.N. Bakhshi, J.F. Mathews, and R.L. Eager, Catalytic Conversion of Canola Oil to Fuels and Chemical Feedstocks, Part I. Effect of Process Conditions on the Performance of HZSM-5 Catalyst, *Can. J. Chem. Eng. 64*:278–284 (1986).
13. Katikaneni, S.P.R., J.D. Adjaye, and N.N. Bakhshi, Catalytic Conversion of Canola Oil to Fuels and Chemicals over Various Catalysts, *Ibid. 33*:484–497 (1995).
14. Katikaneni, S.P.R., J.D. Adjaye, and N.N. Bakhshi, Studies on the Catalytic Conversion of Canola Oil to Hydrocarbons: Influence of Hybrid Catalysts and Steam, *Energy Fuels 9*:599–609 (1995).
15. Prasad, Y.S., and N.N. Bakhshi, Effect of Pretreatment of HZSM-5 Catalyst on Its Performance in Canola Oil Upgrading, *Appl. Catal. 18*:71–85 (1985).
16. Adjaye, J.D., S.P.R. Katikaneni, and N.N. Bakhshi, Catalytic Conversion of a Bio-Fuel to Hydrocarbons: Effects of Mixtures of HZSM-5 and Silica-Alumina on Product Distribution, *Fuel. Proc. Tech. 48*:115–143 (1996).
17. Katikaneni, S.P.R., J.D. Adjaye, R.O. Idem, and N.N. Bakhshi, Catalytic Conversion of Canola Oil over Potassium-Modified HZSM-5 Catalysts: C_2–C_4 Olefins Production and Model Reaction Studies, *Ind. Eng. Chem. Res. 35*:3332–3346 (1995).
18. Katikaneni, S.P.R., J.D. Adjaye, and N.N. Bakhshi, Conversion of Canola Oil to Various Hydrocarbons over Pt/HZSM-5 Bifunctional Catalyst, *Can. J. Chem. Eng. 75*:391–401 (1997).
19. Idem, R.O., S.P.R. Katikaneni, and N.N. Bakhshi, Thermal Cracking of Canola Oil: Reaction Products in the Presence and Absence of Steam, *Energy Fuels 10*:1150–1162 (1996).
20. Idem, R.O., S.P.R. Katikaneni, and N.N. Bakhshi, Catalytic Conversion of Canola Oil to Fuels and Chemicals: Roles of Catalyst Acidity, Basicity and Shape Selectivity on Product Distribution, *Fuel Proc Tech. 51*:101–125 (1997).
21. Billaud, F., V. Dominiguez, P. Broutin, and C. Busson, Production of Hydrocarbons by Pyrolysis of Methyl Esters from Rapeseed Oil, *J. Am. Oil Chem. Soc. 72*:1149–1154 (1995).
22. Gillet-Dominiguez, V., Chemical Upgrading by Pyrolysis of Rapeseed Oil Methyl Esters, Ph.D. Thesis, INPL-ENSIC, University of Nancy, 1994.
23. Gary, J.H., and G.E. Handwerk, *Petroleum Refining, Technology and Economics,* Marcel Dekker, Inc., New York, 1984.
24. Kunii, D., and O. Levenspiel, *Fluidization Engineering*, Butterworth-Heinemann, Massachusetts, 1991.
25. Rase, F.R., *Chemical Reactor Design for Process Plants: Vol 1. Principles and Techniques*, John Wiley, Toronto, 1977.
26. Froment, G.F., and K.B. Bischoff, *Chemical Reactor Analysis and Design*, John Wiley, Toronto, 1979.
27. Ackman R.J., Rapeseed Oil: Chemical and Physical Characteristics, *Rapeseed Association of Canada 45*:12 (1977).
28. Chen, N.Y., J.N. Miale, and W.J. Reagan, Preparation of Zeolites: Example 5, U.S. Patent 4,112,056 (1973).
29. *Micromeritics ASAP 2000 Installation Guide*, Micromeritics Instrument Corporation, Norcross, GA, 1991.
30. Nayak, V.S., and V.R. Choudhary, Isomerization of M-Xylene on HZSM-5, *Appl. Catal. 4*:333–352 (1982).

[Received December 2, 1996; accepted August 11, 1997]